Jet Origin Identification
&
Quantum-based Jet Clustering

朱永峰
PKU

2024.07.09

28th Mini-workshop on the frontier of LHC

Motivation:

1, Quarks and gluons carry color charge, and they can not travel freely. Once generated in high-energy collisions, quarks, and gluon would fragment into numerous particles, which are called jet.

2, ~70% of Z, W, and Higgs bosons decay into double-jet.

Contents:

1. Jet Origin Identification (JOI)
2. Application of Quantum Approximate Optimization Algorithm to Jet Clustering

Jet Origin Identification

categorizes jets into 5 quarks (b, c, s, u, d), 5 anti-quark ($\bar{b}, \bar{c}, \bar{s}, \bar{u}, \bar{d}$), and gluon
= jet flavor tagging + jet charge measurement + s-quark tagging + gluon finding.

PHYSICAL REVIEW LETTERS **132,** 221802 (2024)

Jet-Origin Identification and Its Application at an Electron-Positron Higgs Factory

Hao Liang,[1,2,*] Yongfeng Zhu,[3,*] Yuexin Wang,[1,4] Yuzhi Che,[1,2] Manqi Ruan,[1,2,†]
Chen Zhou,[3,‡] and Huilin Qu[5,§]
[1]*Institute of High Energy Physics, Chinese Academy of Sciences, 19B Yuquan Road, Shijingshan District, Beijing 100049, Chi*
[2]*University of Chinese Academy of Sciences, 19A Yuquan Road, Shijingshan District, Beijing 100049, China*
[3]*State Key Laboratory of Nuclear Physics and Technology, School of Physics, Peking University, Beijing 100871, China*
[4]*China Center of Advanced Science and Technology, Beijing 100190, China*
[5]*CERN, EP Department, CH-1211 Geneva 23, Switzerland*

(Received 16 October 2023; revised 26 April 2024; accepted 1 May 2024; published 31 May 2024)

To enhance the scientific discovery power of high-energy collider experiments, we propose and realize the concept of jet-origin identification that categorizes jets into five quark species (b, c, s, u, d), five antiquarks $(\bar{b}, \bar{c}, \bar{s}, \bar{u}, \bar{d})$, and the gluon. Using state-of-the-art algorithms and simulated $\nu\bar{\nu}H, H \to jj$ events at 240 GeV center-of-mass energy at the electron-positron Higgs factory, the jet-origin identification simultaneously reaches jet flavor tagging efficiencies ranging from 67% to 92% for bottom, charm, and strange quarks and jet charge flip rates of 7%–24% for all quark species. We apply the jet-origin identification to Higgs rare and exotic decay measurements at the nominal luminosity of the Circular Electron Positron Collider and conclude that the upper limits on the branching ratios of $H \to s\bar{s}, u\bar{u}, d\bar{d}$ and $H \to sb, db, uc, ds$ can be determined to 2×10^{-4} to 1×10^{-3} at 95% confidence level. The derived upper limit for $H \to s\bar{s}$ decay is approximately 3 times the prediction of the standard model.

DOI: 10.1103/PhysRevLett.132.221802

Eur. Phys. J. C (2024) 84:152
https://doi.org/10.1140/epjc/s10052-024-12475-5

THE EUROPEAN PHYSICAL JOURNAL C

Check for updates

Regular Article - Experimental Physics

ParticleNet and its application on CEPC jet flavor tagging

Yongfeng Zhu[1,a], **Hao Liang**[2,3], **Yuexin Wang**[2,3], **Huilin Qu**[4], **Chen Zhou**[1,b], **Manqi Ruan**[2,3,c]
[1] State Key Laboratory of Nuclear Physics and Technology, School of Physics, Peking University, Beijing 100871, China
[2] Institute of High Energy Physics, Chinese Academy of Sciences, Beijing 100049, China
[3] University of Chinese Academy of Sciences (UCAS), Beijing 100049, China
[4] EP Department, CERN, 1211 Geneva 23, Switzerland

Received: 15 November 2023 / Accepted: 23 January 2024

Abstract Quarks (except top quarks) and gluons produced in collider experiments hadronize and fragment into sprays of stable particles, called jets. Identification of quark flavor is desired for collider experiments in high-energy physics, relying on flavor tagging algorithms. In this study, using a full simulation of the Circular Electron Positron Collider (CEPC), we investigate the flavor tagging performance of two different algorithms: ParticleNet, based on a Graph Neural Network, and LCFIPlus, based on the Gradient Booted Decision Tree. Compared to LCFIPlus, ParticleNet significantly enhances flavor tagging performance, resulting in a significant improvement in benchmark measurement accuracy, i.e., a 36% improvement for $\sigma(ZH) \cdot Br(Z \to \nu\bar{\nu}, H \to c\bar{c})$ measurement and a 75% improvement for $|V_{cb}|$ measurement via W boson decay, respectively, when the CEPC operates as a Higgs factory at the center-of-mass energy of 240 GeV and collects an integrated luminosity of 5.6 ab^{-1}. We compare the performance of ParticleNet and LCFIPlus at different vertex detector configurations, observing that the inner radius is the most sensitive parameter, followed by material budget and spatial resolution.

light on the properties of massive SM particles and is critical for experimental exploration at the high-energy frontier. Flavor tagging is used to distinguish jets which hadronize from quarks of different flavors or from gluons. To promote the development of future electron-positron Higgs factories, which is regarded as a high priority future collider [4], accurate performance analysis and optimization of both detectors and algorithms are essential. Jet flavor tagging and relevant benchmark analyses serve as good objectives.

The Circular Electron Positron Collider (CEPC) [5] is a large-scale collider facility that was proposed after the discovery of the Higgs boson in 2012. It is designed to have a circumference of 100 km with two interaction points. It will be able to operate at multiple center-of-mass energies, including 240 GeV as a Higgs factory, 160 GeV for a W^+W^- threshold scan, and 91 GeV as a Z factory. It also can be upgraded to 360 GeV for a $t\bar{t}$ threshold scan. Table 1 summarizes its baseline operating scheme and the corresponding boson yield predictions [6]. One of the main scientific objectives of the CEPC is the precise measurement of properties of the Higgs boson. Additionally, trillions of $Z \to q\bar{q}$ events can provide

PhysRevLett.132.221802 | Eur. Phys. J. C (2024) 84:152

jet represented as :

Construct GNN
with “message passing”

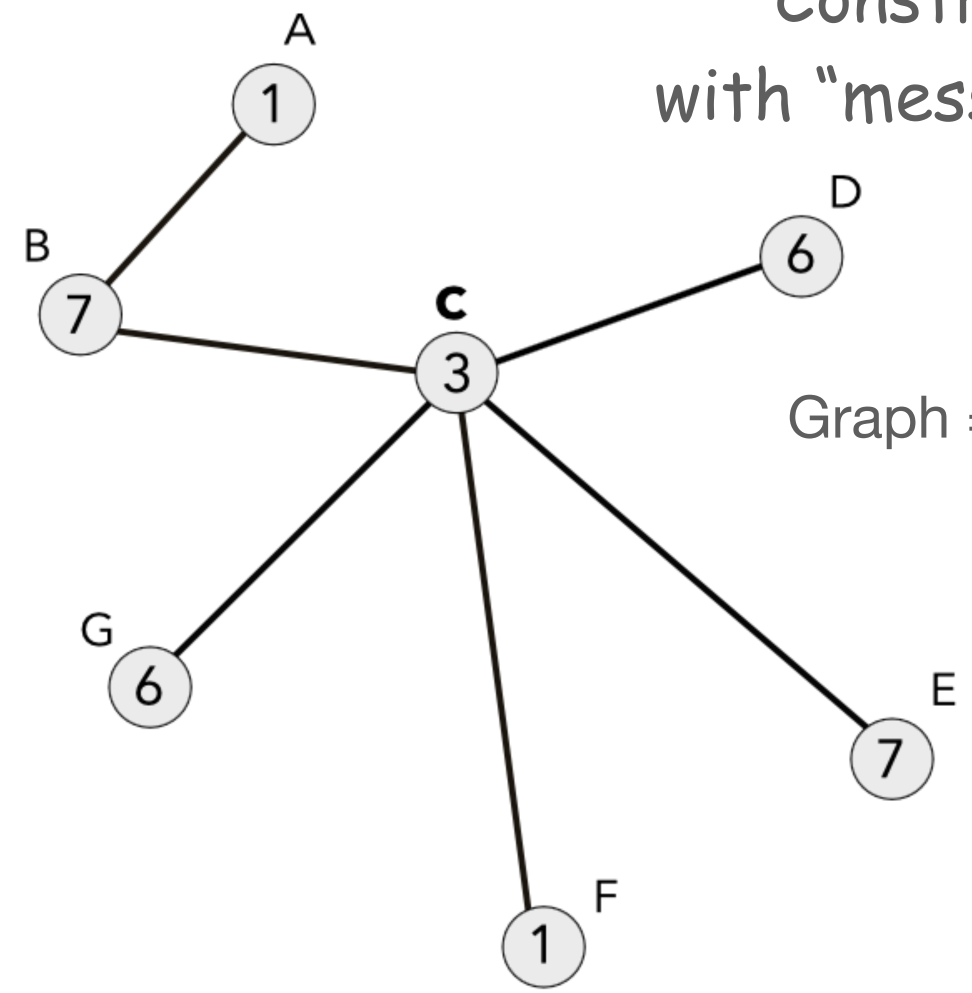

Graph = (Vertices, Edges)

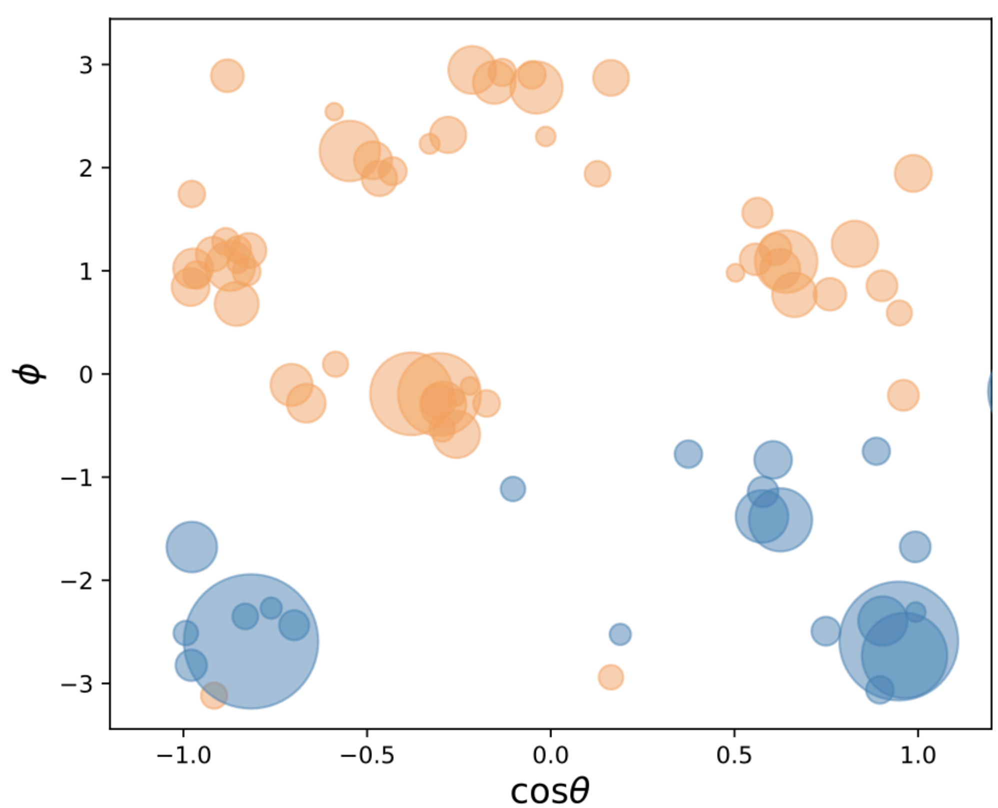

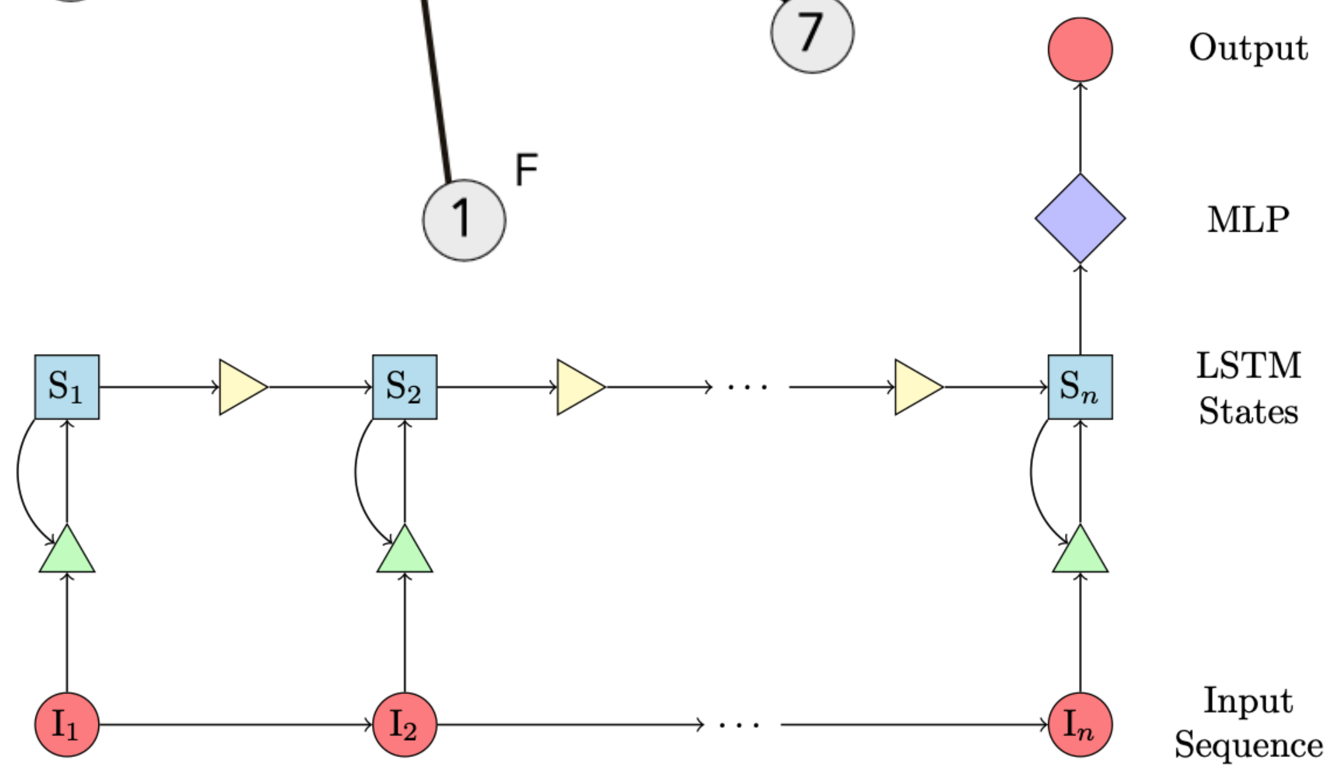

FIG. 4: Architecture of the Long Short Term Memory networks as described in the text.

arXiv:1607.08633

Samples

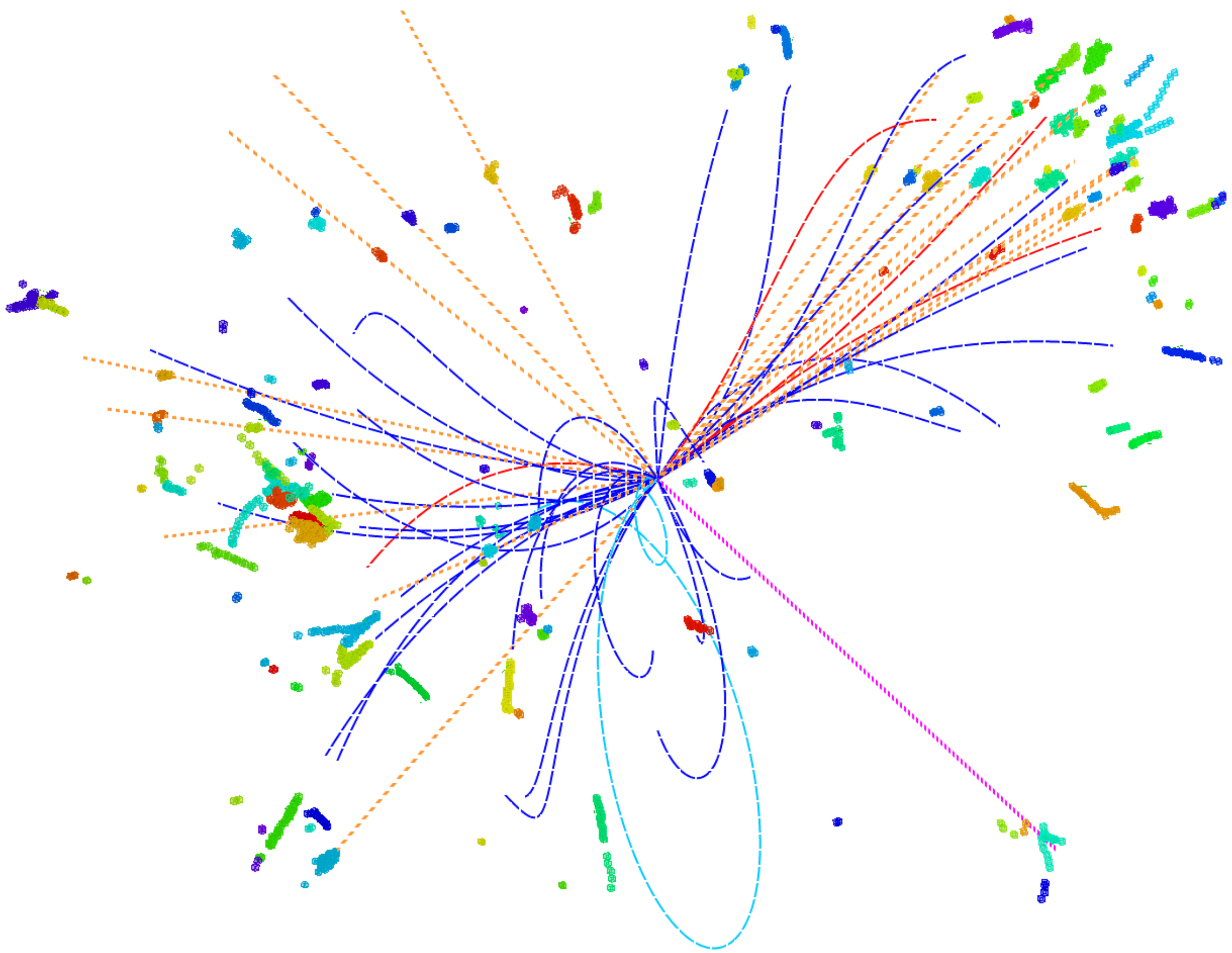

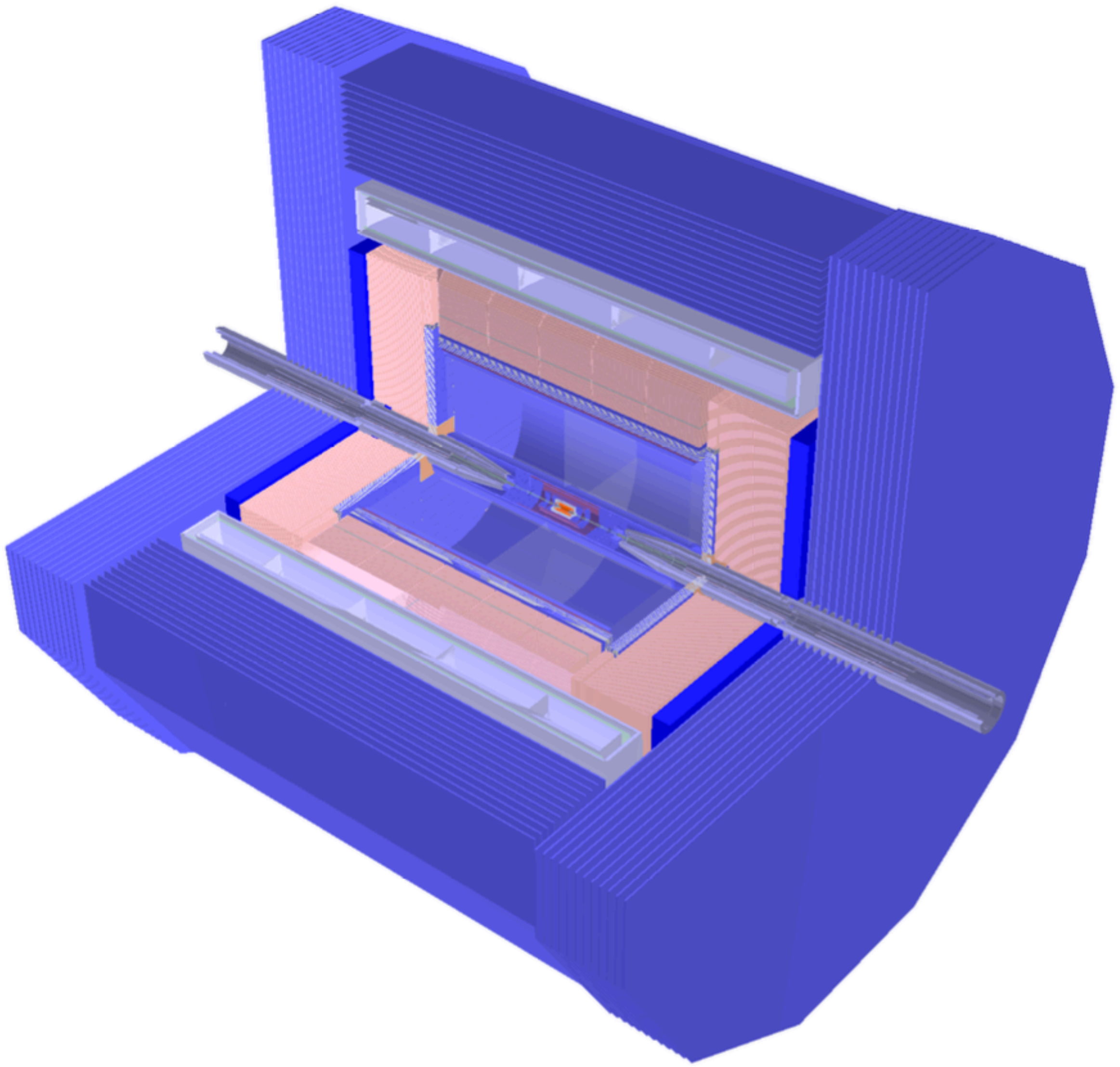

Full Simulated vvH, Higgs to two jets sample at CEPC baseline configuration: CEPC-v4 detector,

1 Million samples each, 60/20/20% for training, validation & test

the ParticleNet and input features

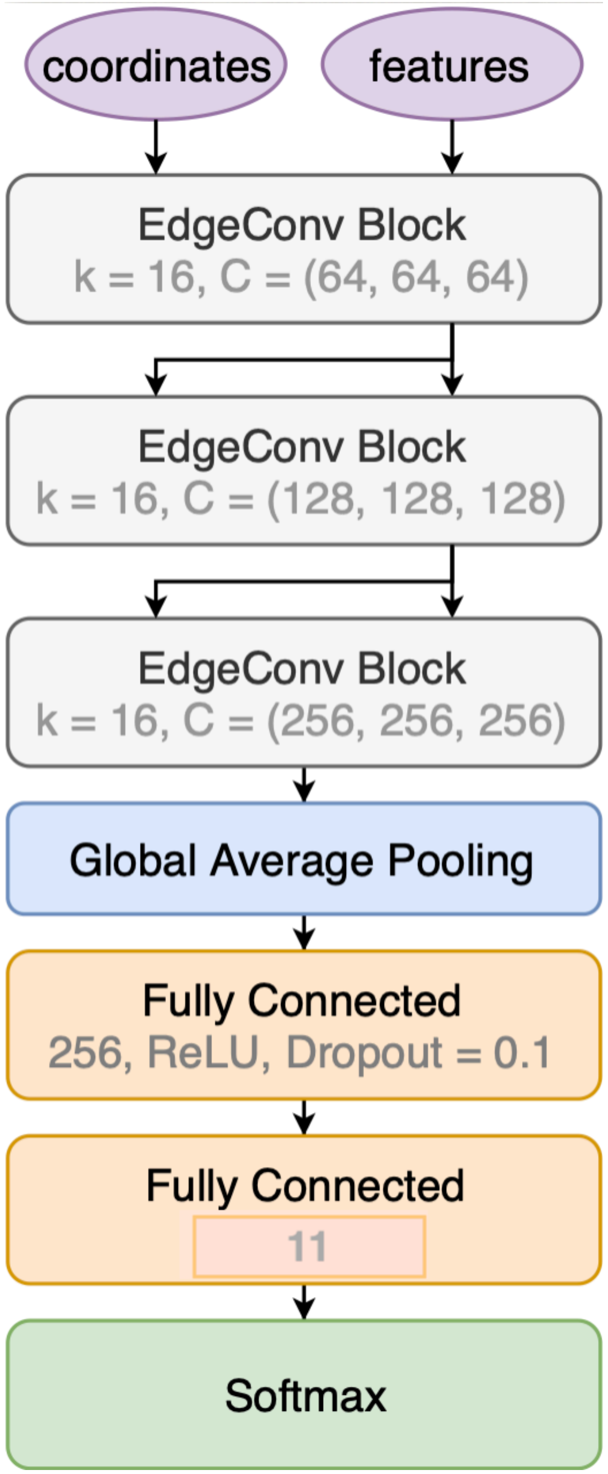

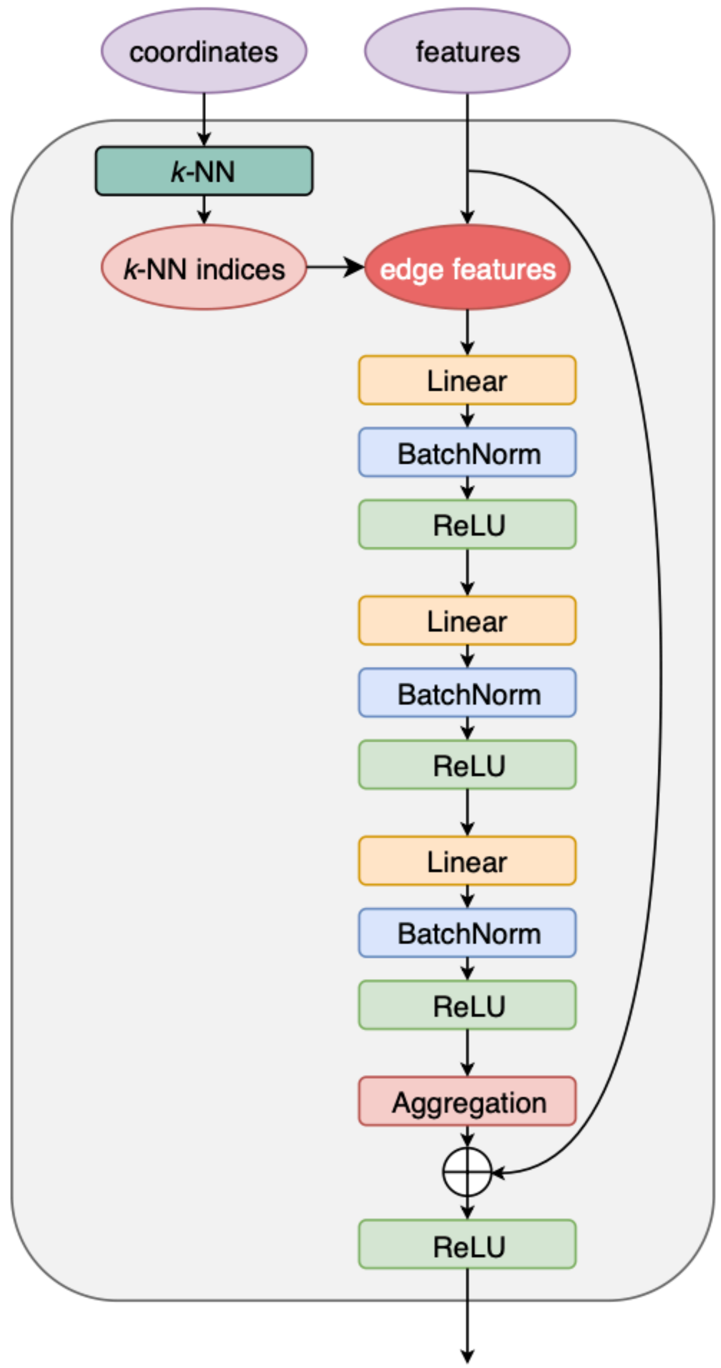

input features :

Table 3 The input variables used in ParticleNet for jet flavor tagging at the CEPC

Variable	Definition
$\Delta\,\eta$	Difference in pseudorapidity between the particle and the jet axis
$\Delta\,\phi$	Difference in azimuthal angle between the particle and the jet axis
$\log P_t$	Logarithm of the particle's P_t
logE	Logarithm of the particle's energy
$\log \frac{P_t}{P_t(jet)}$	Logarithm of the particle's P_t relative to the jet P_t
$\log \frac{E}{E(jet)}$	Logarithm of the particle's energy relative to the jet energy
ΔR	Angular separation between the particle and the jet axis
d_0	Transverse impact parameter of the track
$d_0$err	Uncertainty associated with the measurement of the d_0
z_0	Longitudinal impact parameter of the track
$z_0$err	Uncertainty associated with the measurement of the z_0
Charge	Electric charge of the particle
isElectron	Whether the particle is an electron
isMuon	Whether the particle is a muon
isChargedKaon	Whether the particle is a charged Kaon
isChargedPion	Whether the particle is a charged Pion
isProton	Whether the particle is a proton
isNeutralHadron	Whether the particle is a neutral hadron
isPhoton	Whether the particle is a photon

Phys. Rev. D 101, 056019

the performance of jet origin identification

ParticleNet algorithm attaches each jet with 11 likelihoods corresponding to 11 types of jets.
Then the jet type is determined according to the maximum likelihood.

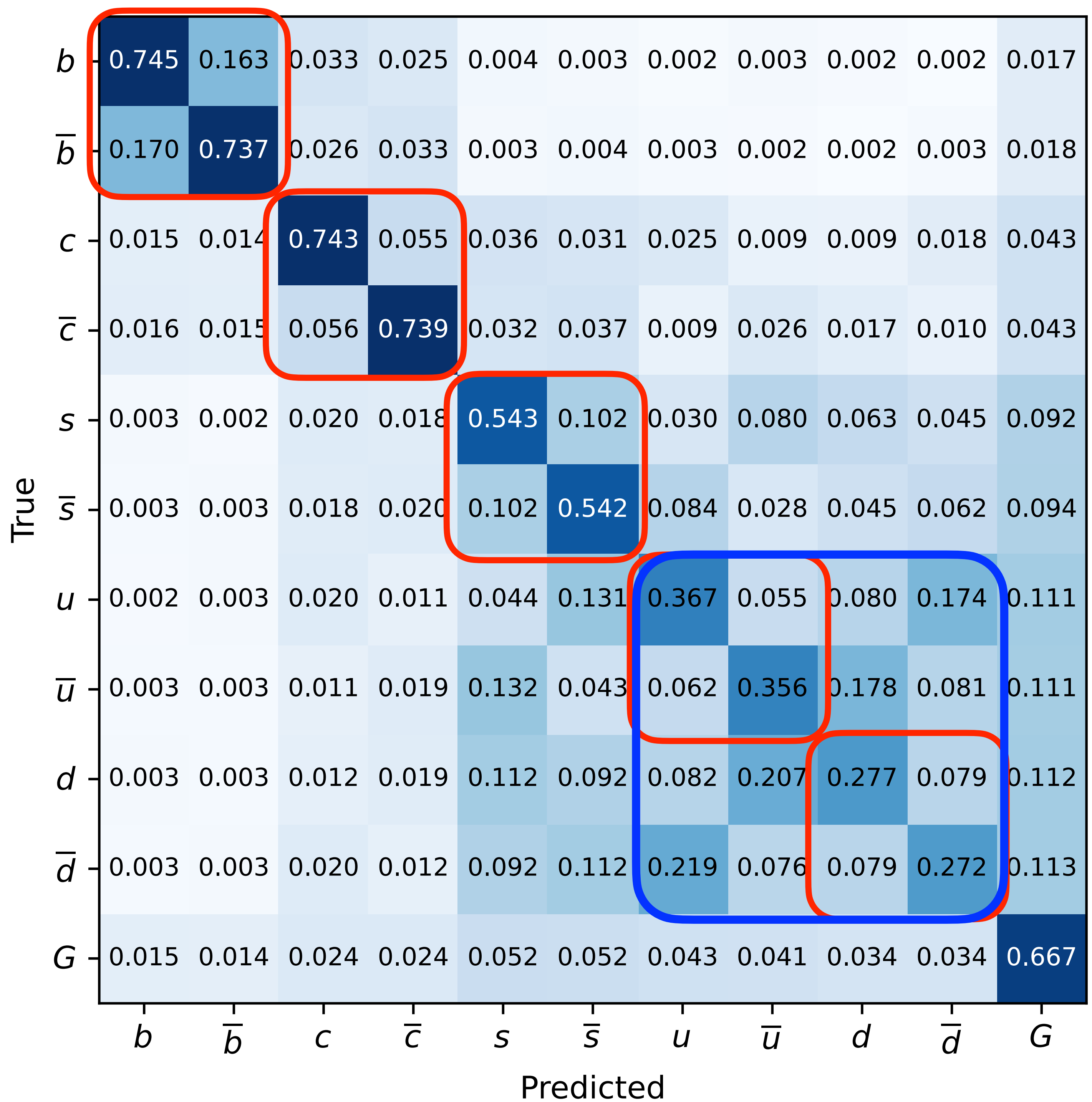

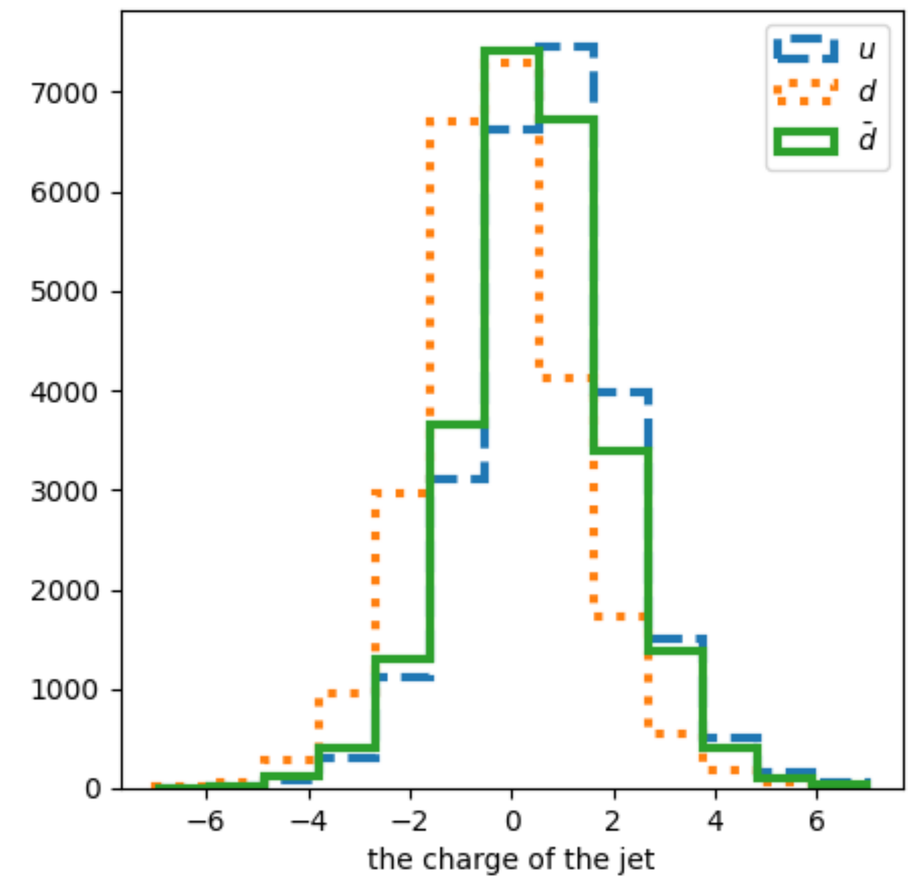

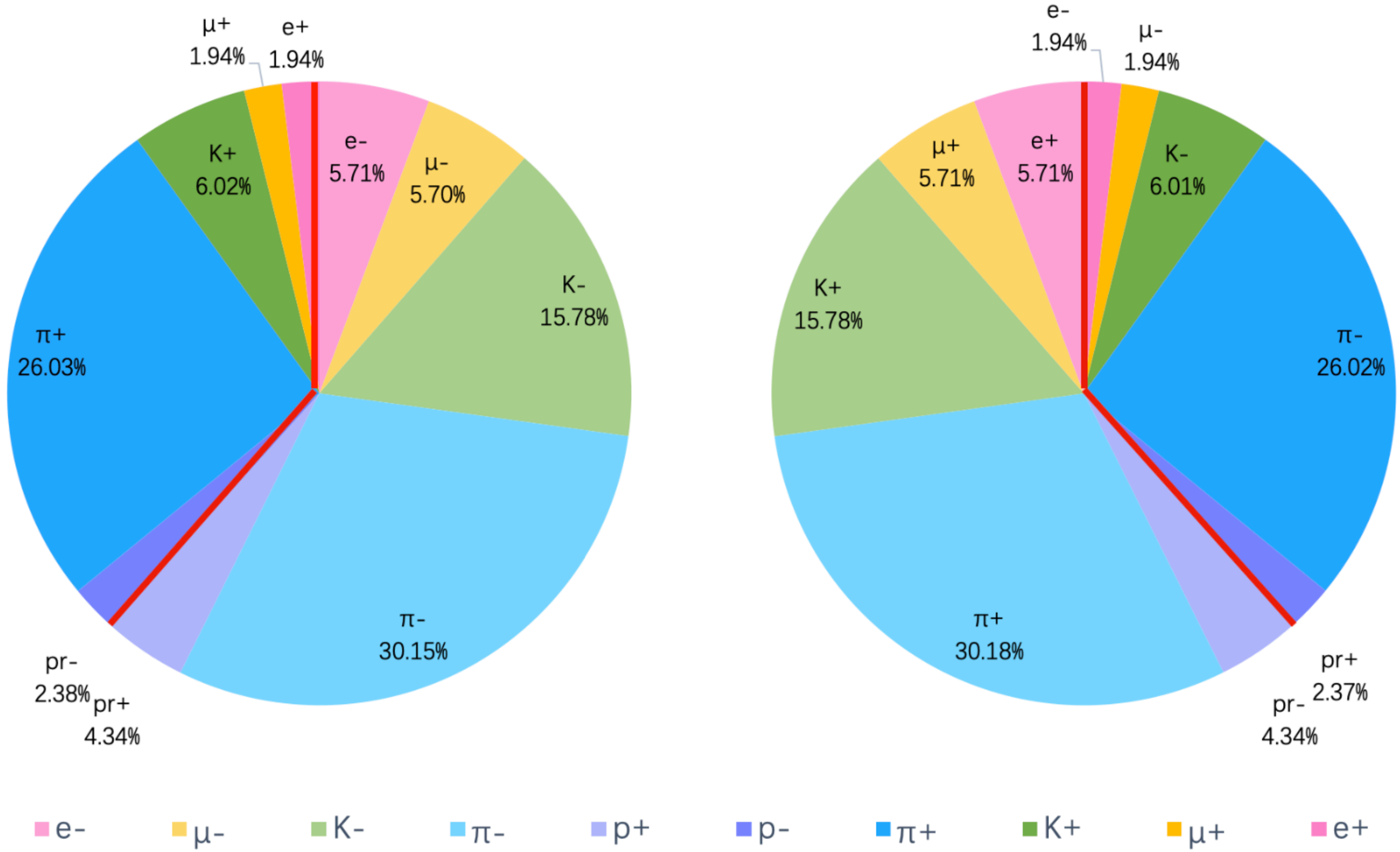

Figure 5. The percentages of species of final state leading charged particles within the b jet (left) and the $\bar{b}$ jet (right) by WHIZARD 1.95.

arXiv:2306.14089

the performance of jet origin identification

jet flavor is defined as $max(b+\bar{b},\ c+\bar{c},\ s+\bar{s},\ u+\bar{u},\ d+\bar{d},\ g)$

jet charge is assigned by comparing the quark and anti-quark likelihoods of the corresponding flavor

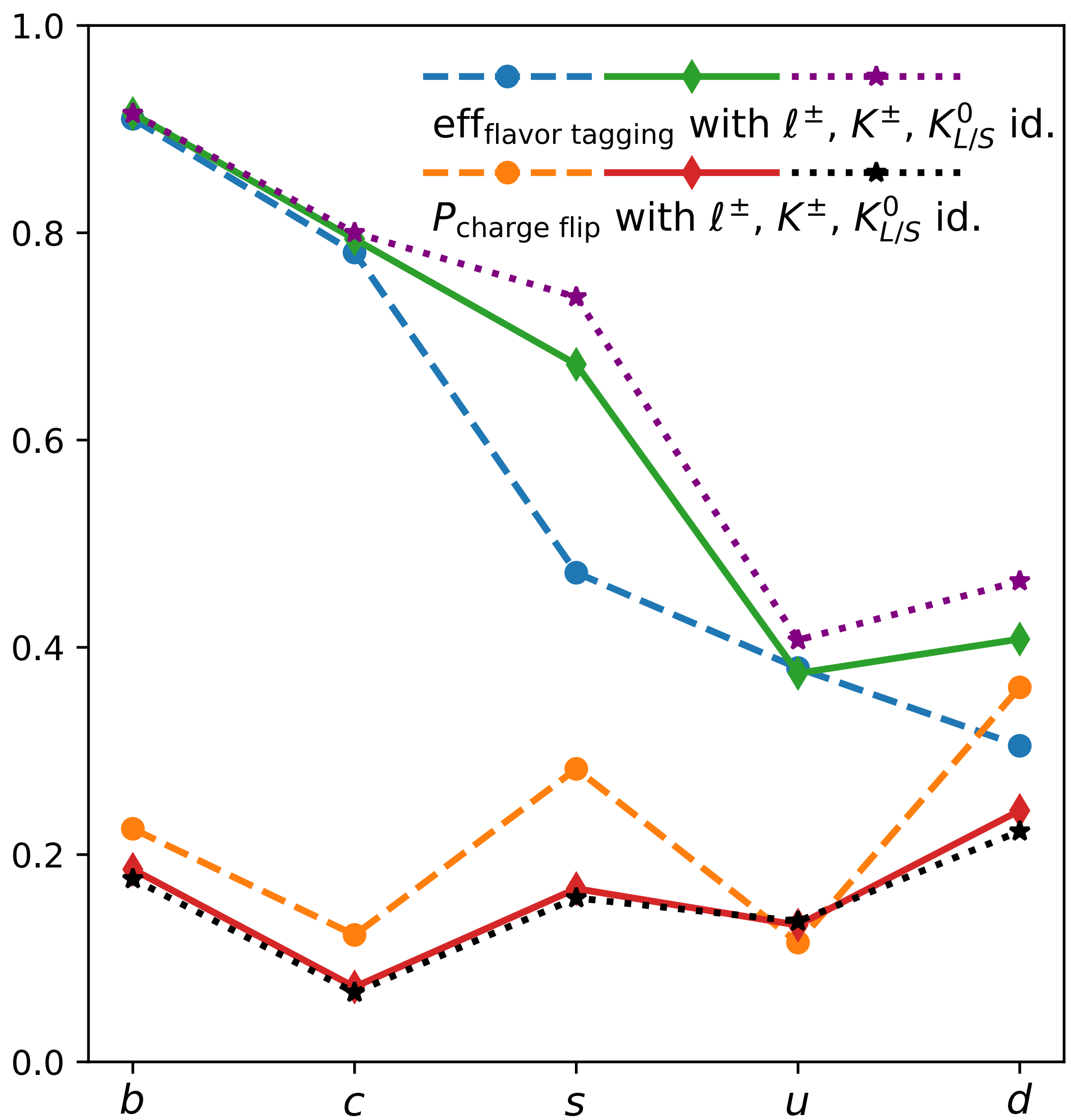

To understand the impact of PID, three scenarios are compared.

1, assumes perfect identification of charged leptons ($\ell^{\pm}$)

2, further assumes perfect identification of the charged hadrons ($K^{\pm}$)

3, on top of the second scenario, assumes perfect identification of K_L and K_S.

default scenario: 2 scenario, based on:

Eur. Phys. J. C 80, 7 (2020)

Journal of Instrumentation 16, P06013 (2021)

Eur. Phys. J. C 78, 464 (2018)

Eur. Phys. J. C 83, 93 (2023)

Nucl. Instrum. Meth. A 1047, 167835 (2023)

Benchmark physics analyses

Begin with the existing analyses of $\nu\bar{\nu}H, H \to b\bar{b}/c\bar{c}/gg$, (arXiv:2203.01469) and combining the jet origin identification, we obtain the upper limits on branching ratios of seven Higgs rare and FCNC hadronic decay modes.

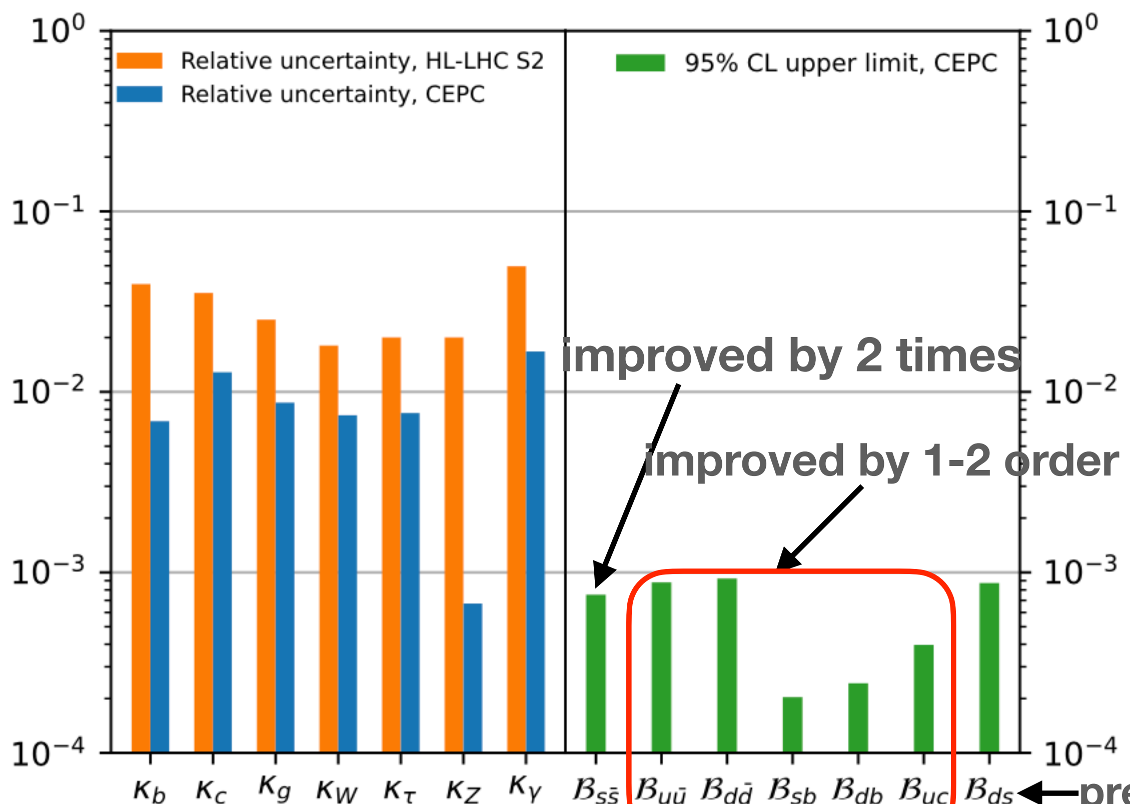

FIG. 5. Expected upper limits on the branching ratios of rare Higgs boson decays from this Letter (green) and the relative uncertainties of Higgs couplings anticipated at CEPC [19] (blue) and HL-LHC [43] (orange) under the kappa-0 fit scenario [54] and scenario S2 of systematics [55], as cited in Ref. [19]. The limit on $B_{s\bar{s}}$ corresponds to an upper limit of 1.7 on the Higgs-strange coupling modifier κ_s (not shown).

TABLE I. Summary of background yields from $H \to b\bar{b}/c\bar{c}/gg$, Z, and W prior to the flavor-based event selection, along with the expected upper limits on Higgs decay branching ratios at 95% CL under the background-only hypothesis.

	Bkg (10^3)			Upper limits on Br (10^{-3})						
	H	Z	W	$s\bar{s}$	$u\bar{u}$	$d\bar{d}$	sb	db	uc	ds
$\nu\bar{\nu}H$	151	20	2.1	0.81	0.95	0.99	0.26	0.27	0.46	0.93
$\mu^+\mu^-H$	50	25	0	2.6	3.0	3.2	0.5	0.6	1.0	3.0
e^+e^-H	26	16	0	4.1	4.6	4.8	0.7	0.9	1.6	4.3
Comb.	⋯	⋯	⋯	0.75	0.91	0.95	0.22	0.23	0.39	0.86

[23] J. Duarte-Campderros, G. Perez, M. Schlaffer, and A. Soffer, Phys. Rev. D **101**, 115005 (2020), arXiv:1811.09636 [hep-ph].

[44] A. Albert *et al.*, "Strange quark as a probe for new physics in the higgs sector," (2022), arXiv:2203.07535 [hep-ex].

[53] J. de Blas *et al.*, JHEP **01**, 139 (2020), arXiv:1905.03764 [hep-ph].

[54] J. De Blas, G. Durieux, C. Grojean, J. Gu, and A. Paul, JHEP **12**, 117 (2019), arXiv:1907.04311 [hep-ph].

Comparison between different physics processes

$Z \to q\bar{q}$ at $\sqrt{s} = 91.2\ GeV$
$\nu\bar{\nu}H, H \to q\bar{q}$ at $\sqrt{s} = 240\ GeV$

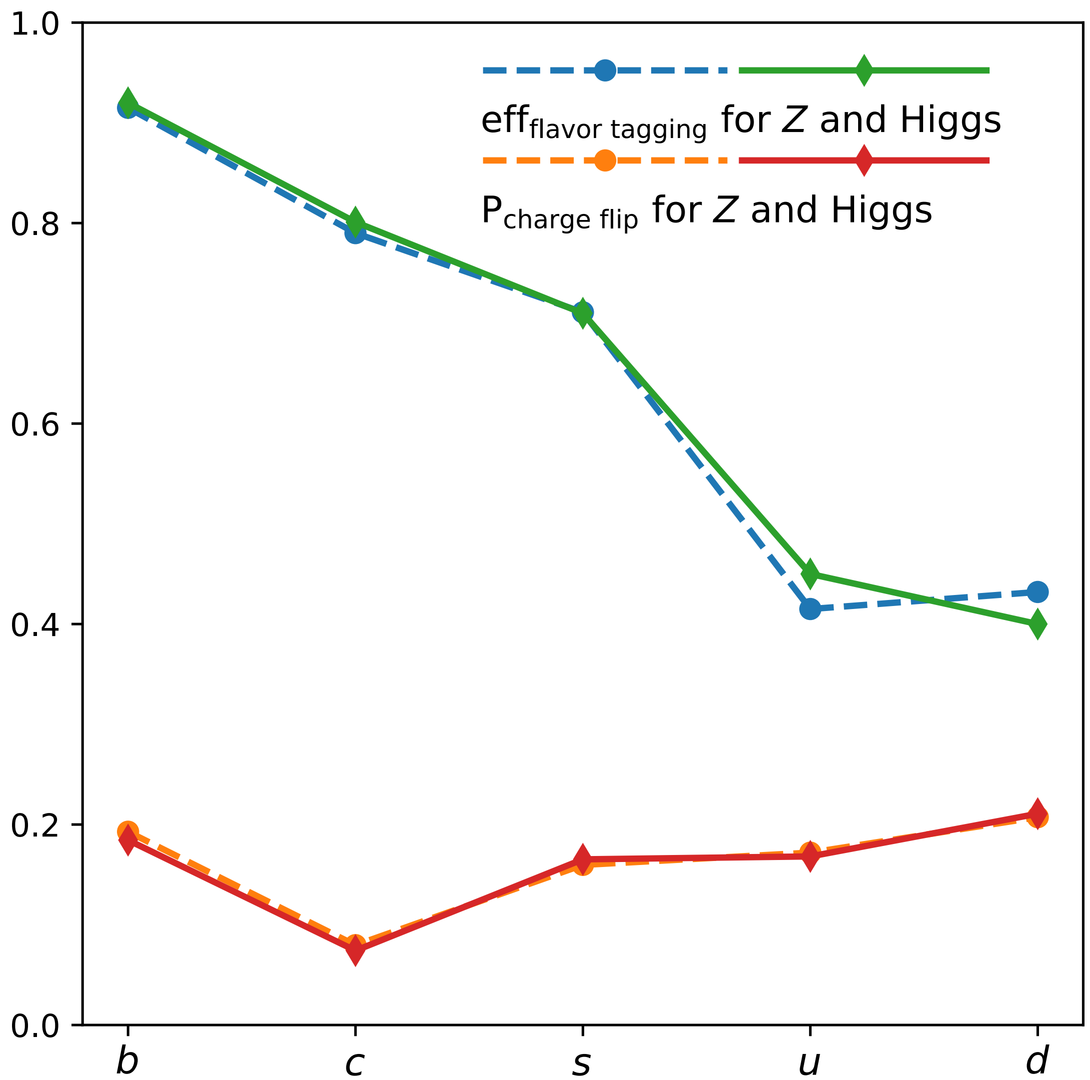

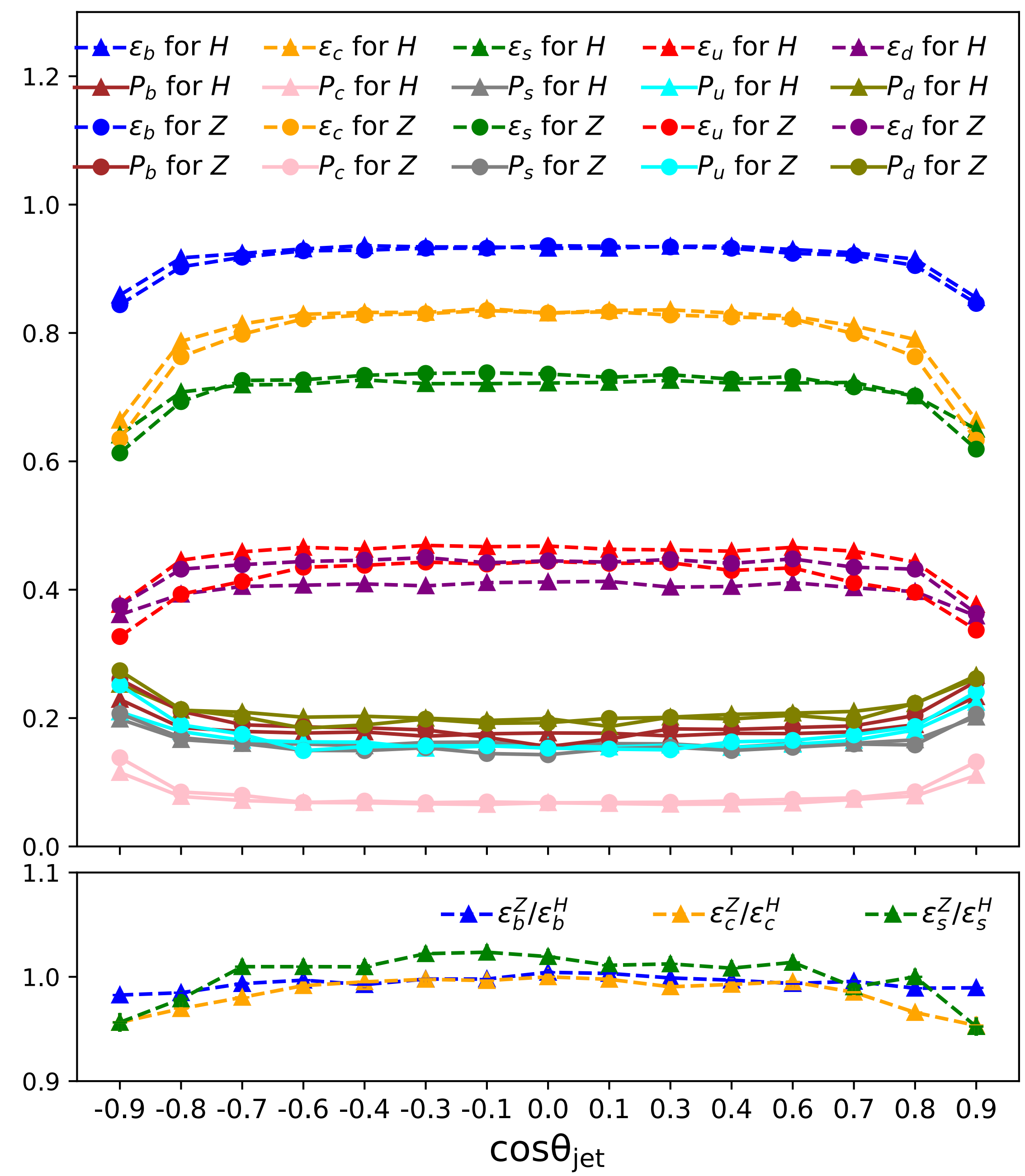

The jet origin identification performance agrees with each other, especially in the fiducial barrel region of the detector for the flavor tagging performance of b, c, and s.

Comparison between different hadronization models

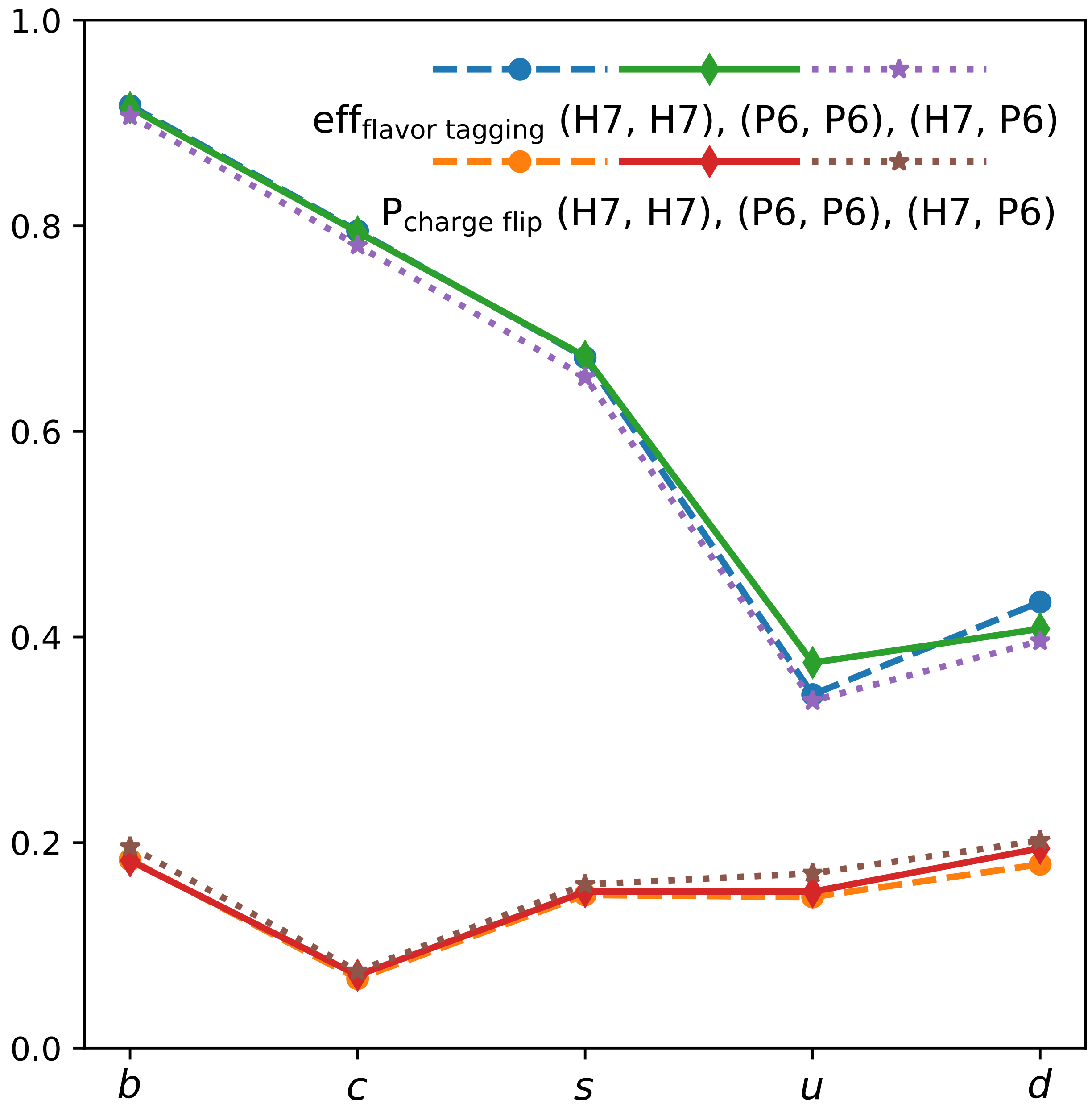

Pythia-6.4
Herwig-7.2.2

$\nu\bar{\nu}H, H \rightarrow jj$ at $\sqrt{s} = 240\ GeV$

(A, B) means: training on A, test on B

The jet origin identificaion performanc agrees with each other, especially for b, c, and s jets, while exhibits small but visible differences for u and d jets.

A Novel Quantum Realization of Jet Clustering in High-Energy Physics Experiments

Yongfeng Zhu[a], WeiFeng Zhuang[b], Chen Qian[b], Yunheng Ma[b], Dong E. Liu[b,c,*], Manqi Ruan[d,e,*], Chen Zhou[a,*]

[a] *State Key Laboratory of Nuclear Physics and Technology, School of Physics, Peking University, Haidian District, Beijing, 100871, China*
[b] *Beijing Academy of Quantum Information Sciences, Haidian District, Beijing, 100193, China*
[c] *Department of Physics, Tsinghua University, Haidian District, Beijing, 100084, China*
[d] *Institute of High Energy Physics, Chinese Academy of Sciences, Shijingshan District, Beijing, 100049, China*
[e] *University of Chinese Academy of Sciences, Shijingshan District, Beijing, 100049, China*

VQA v.s. ML

parameters update

	input	construct	output	cost function
ML	features of samples	model	prediction classification or regression y’	f(y, y’)
VQA	initial state $\lvert\psi(0)\rangle$	quantum circuit	final state $\lvert\psi(\theta)\rangle$	$E(\theta) = \langle\psi(\theta)\lvert H \rvert\psi(\theta)\rangle$

```
- [part_isElectron, null]
- [part_isMuon, null]
- [part_isNeutralHadron, null]
- [part_isPhoton, null]
- [part_d0, null]
- [part_d0err, 0, 1, 0, 1]
- [part_dz, null]
- [part_dzerr, 0, 1, 0, 1]
- [part_deta, null]
- [part_dphi, null]
- [part_pt_log, -1.5, 1.0]
- [part_e_log, -0.687, 1.0]
- [part_logptrel, -4.7, 1.0]
- [part_logerel, -4.473, 1.0]
- [part_deltaR, 2.1, 2.3]
- [part_charge, null]
- [part_isChargedHadron, null]
```

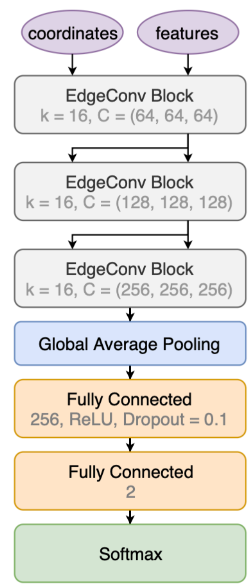

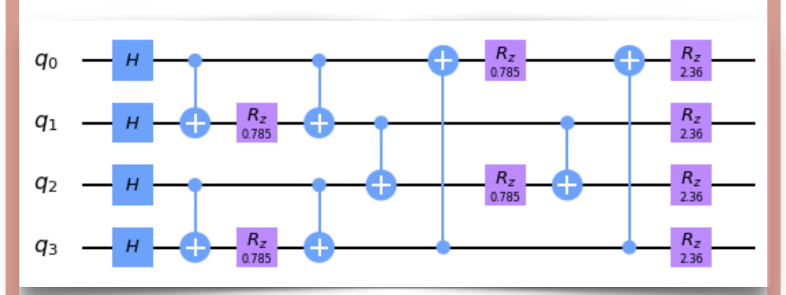

the driver Hamiltonian $H_D : B = \sum_{j=1}^{n} \sigma_j^x$ the problem Hamiltonian $H_P : C = \frac{1}{2} \sum_{(i,j)\in E} W_{ij}(1 - \sigma_i^z \sigma_j^z)$

$$H(t) = (1 - s(t))H_D + s(t)H_P \qquad U(t) = \tau e^{\frac{-i}{\hbar}\int_o^t H(T)dT}$$

AQC

$$U(T,0) = U(T, T - \Delta t)U(T - \Delta t, T - 2\Delta t)\ldots U(\Delta t,0) = \prod_{j=1}^{P} U(j\Delta t, (j-1)\Delta t) \approx \prod_{j=1}^{P} e^{-iH(j\Delta t)\Delta t}$$

$$H(j\Delta t) = (1 - s(j\Delta t))H_D + s(j\Delta t)H_P$$

QAOA

$$U(T,0) \approx \prod_{j=1}^{P} e^{-i(1-s(j\Delta t))H_D\Delta t} e^{-is(j\Delta t)H_P\Delta t} = \prod_{j=1}^{P} U((1 - s(j\Delta t))\Delta t, H_D)U(s(j\Delta t)\Delta t, H_P) = \prod_{j=1}^{P} U(\beta_j, B)U(\gamma_j, C)$$

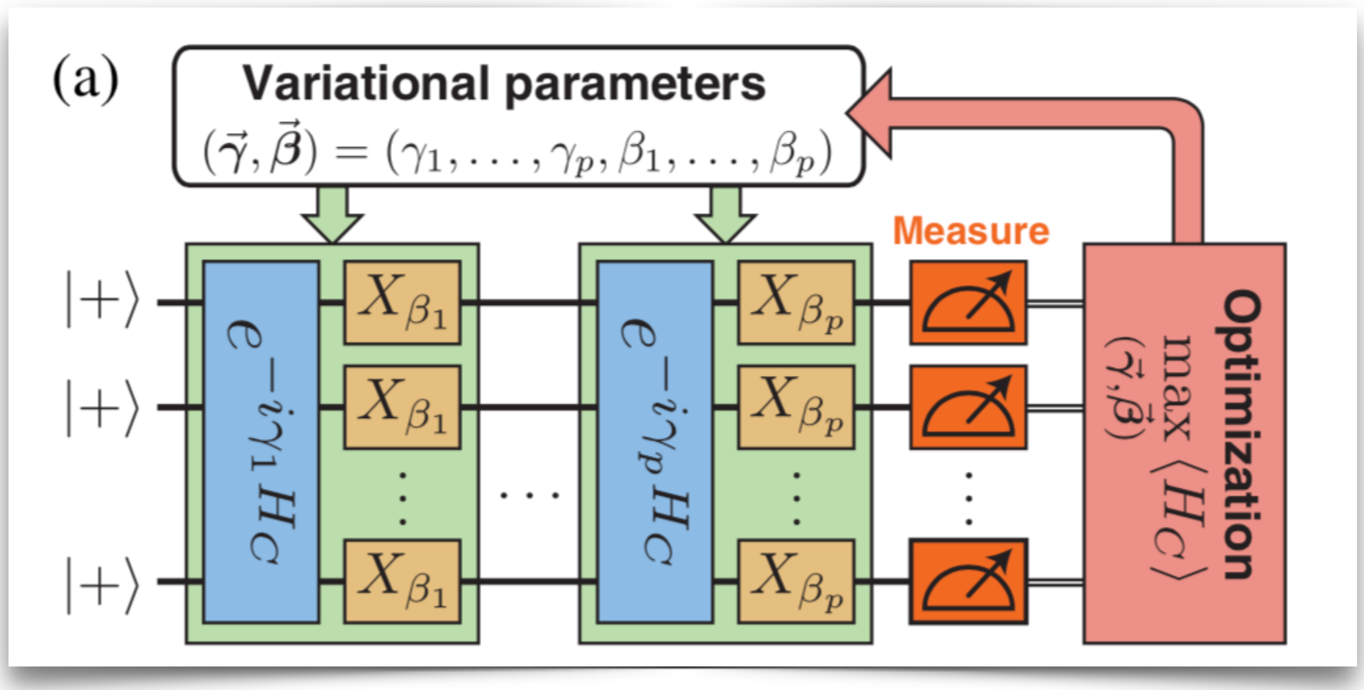

Performance of jet clustering

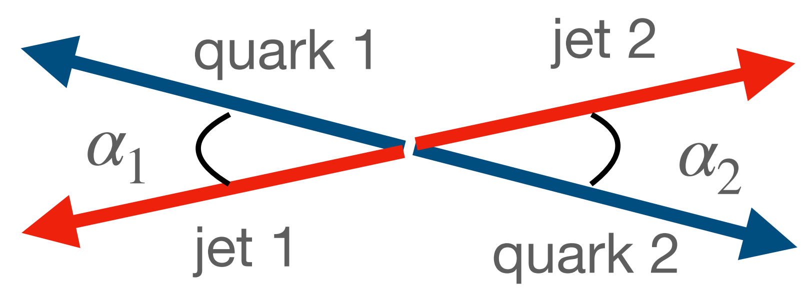

with sample $e^+e^- \to ZH \to \nu\bar{\nu}s\bar{s}$

criterion is $\alpha = \alpha_1 + \alpha_2$

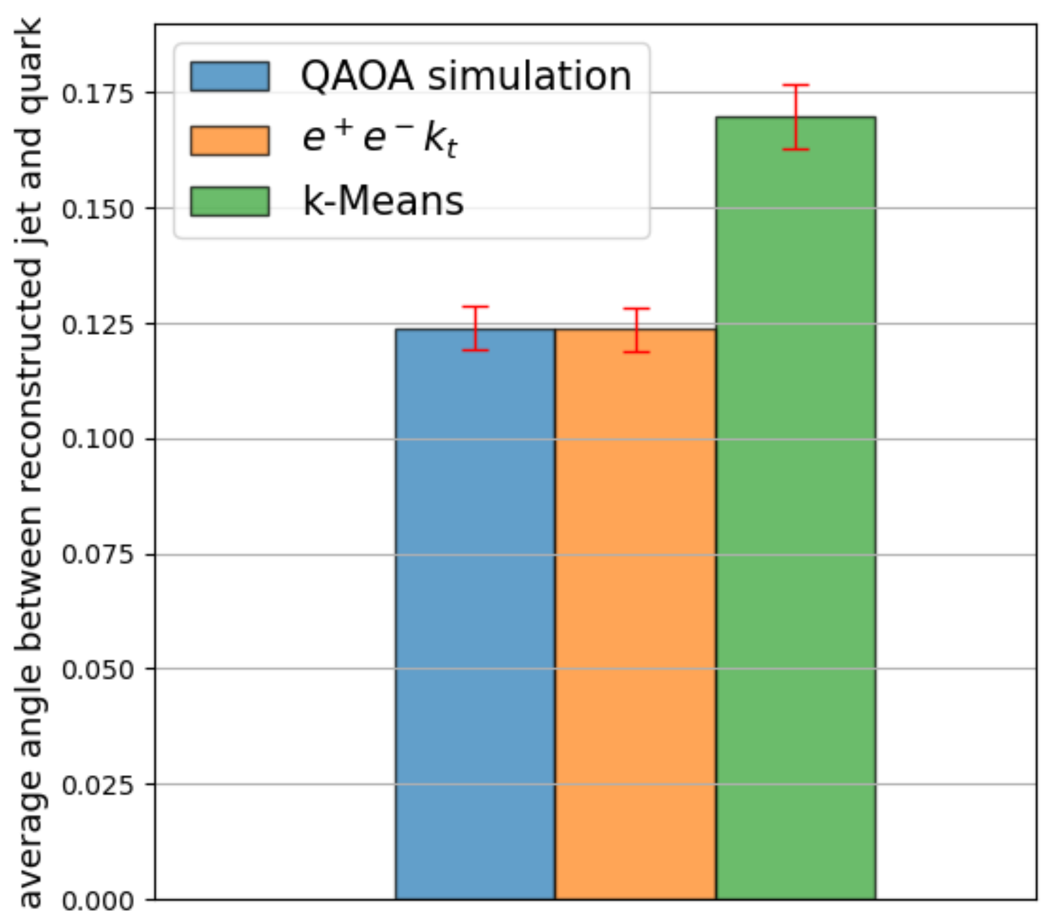

$H \to s\bar{s}$ with 30 final state particles
compare quantum simulator, ee_kt, and k-Means algorithms.

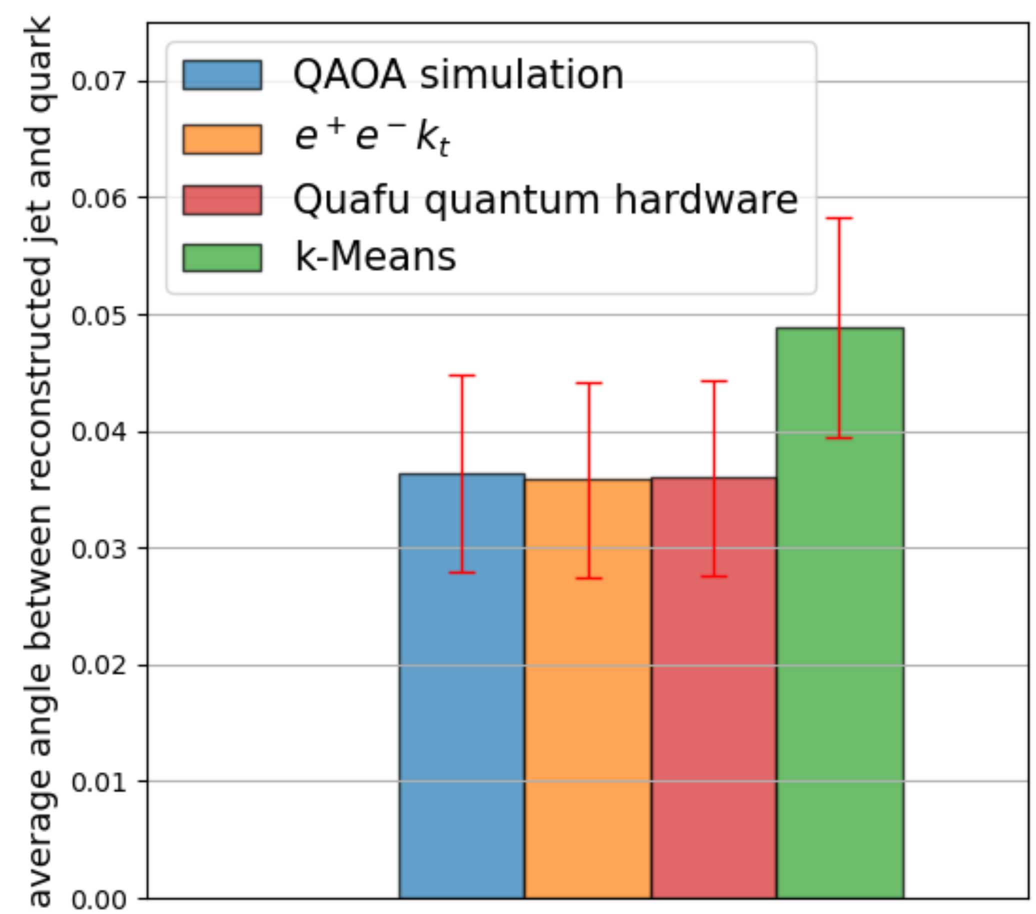

$H \to s\bar{s}$ with 6 final state particles
compare quantum hardware, simulator, ee_kt, and k-Means

Summary

- Both analyses of full hadronic WW/ZZ separation and $H \to b\bar{b}/c\bar{c}/gg$ measurement suggest that the importance of jet clustering and jet flavor tagging.
- We proposed and developed jet origin identification algorithm for jet flavor tagging and jet charge measurement, and achieved significant improvement on the measurement of Higgs rare and FCNC decay .
- We apply a quantum combinatorial optimization algorithm, QAOA, on jet clustering. With Higgs->ss samples, QAOA running on quantum virtual machine and quantum hardware can reach the similar performance to classical jet clustering algorithm, ee_kt.

Many thanks !

Backup

Graph Neural Network

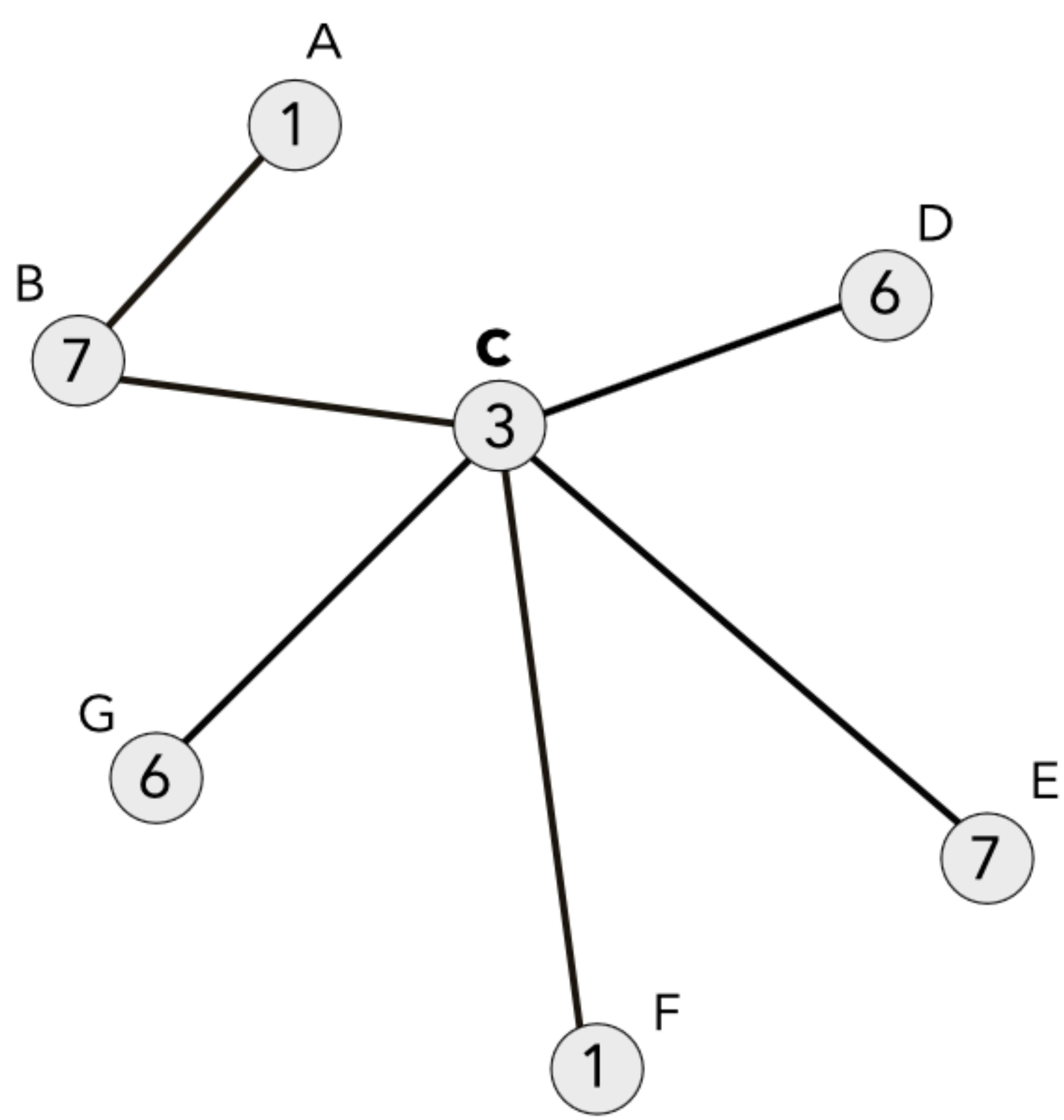

DOI: 10.23915/distill.00032

utilize the “passing-message”, we can perform the following tasks:

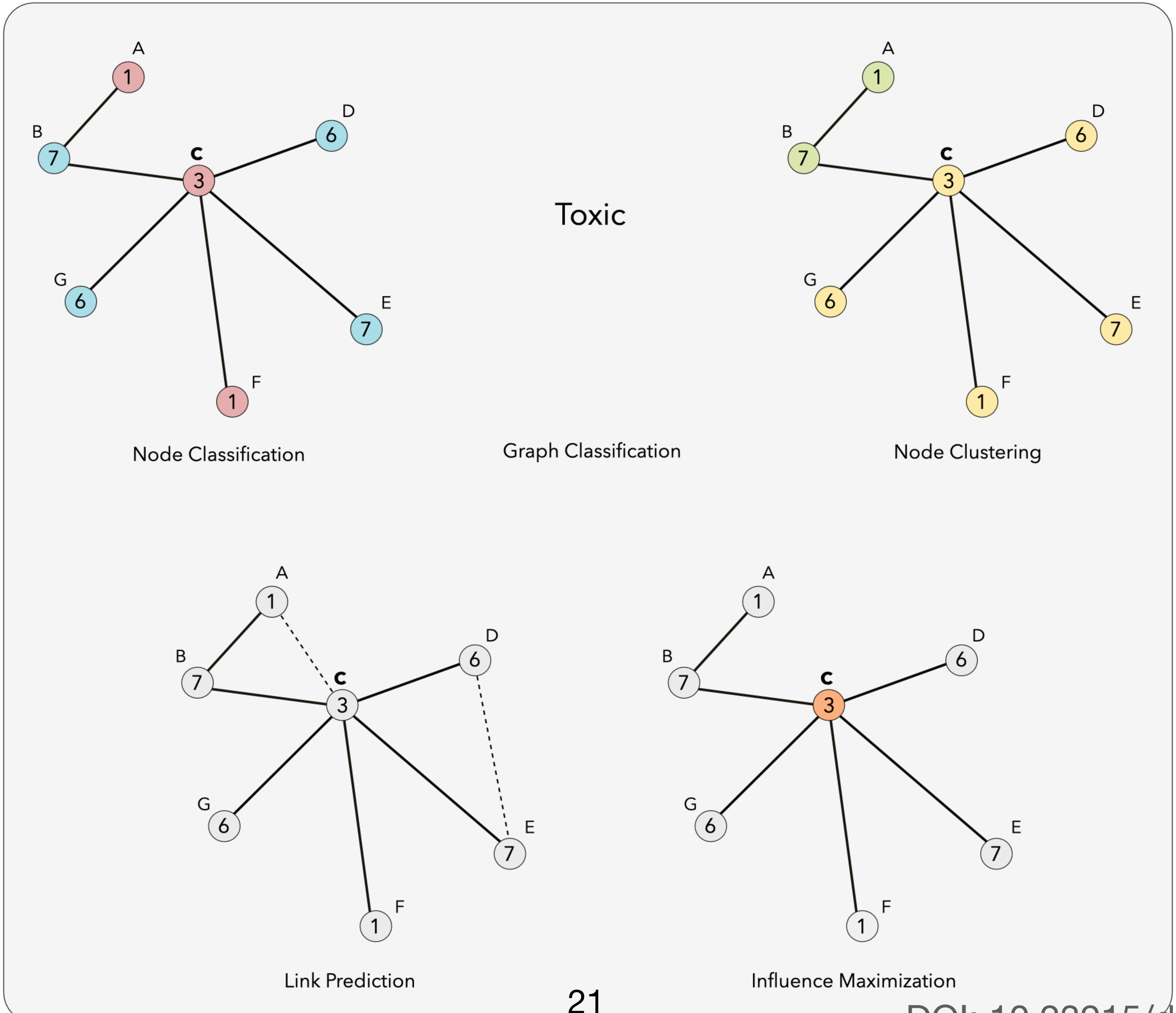

Examples of problems that can be defined over graphs. This list is not exhaustive!

DOI: 10.23915/distill.00032

MLP

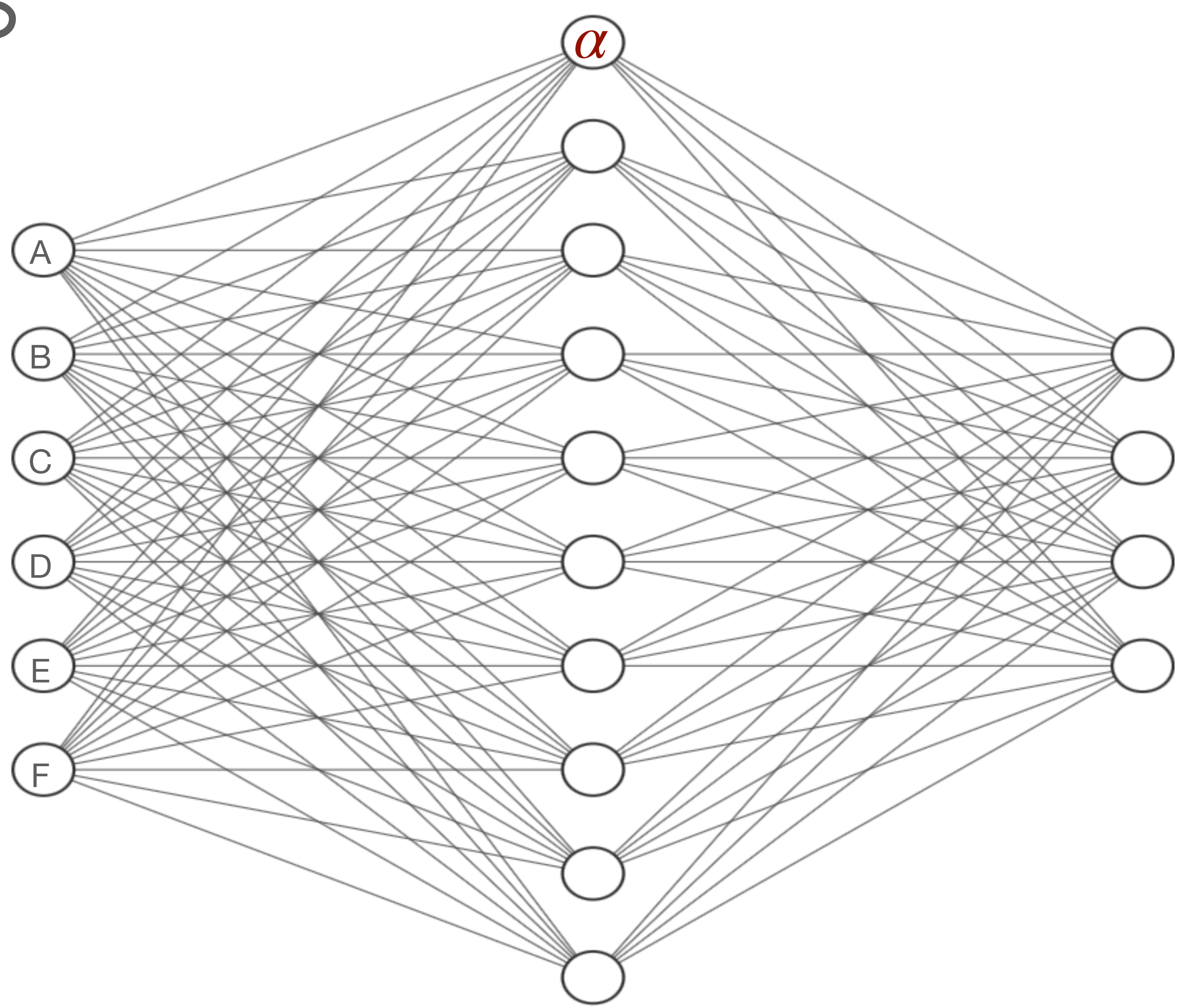

$$\alpha = \sigma(W_1 \cdot A + W_2 \cdot B + W_3 \cdot C + W_4 \cdot D + W_5 \cdot E + W_6 \cdot F)$$

σ: activation function

W: weight, learnable parameter

$$\sum_{u \in N(v)} h_u^{(k-1)} :$$

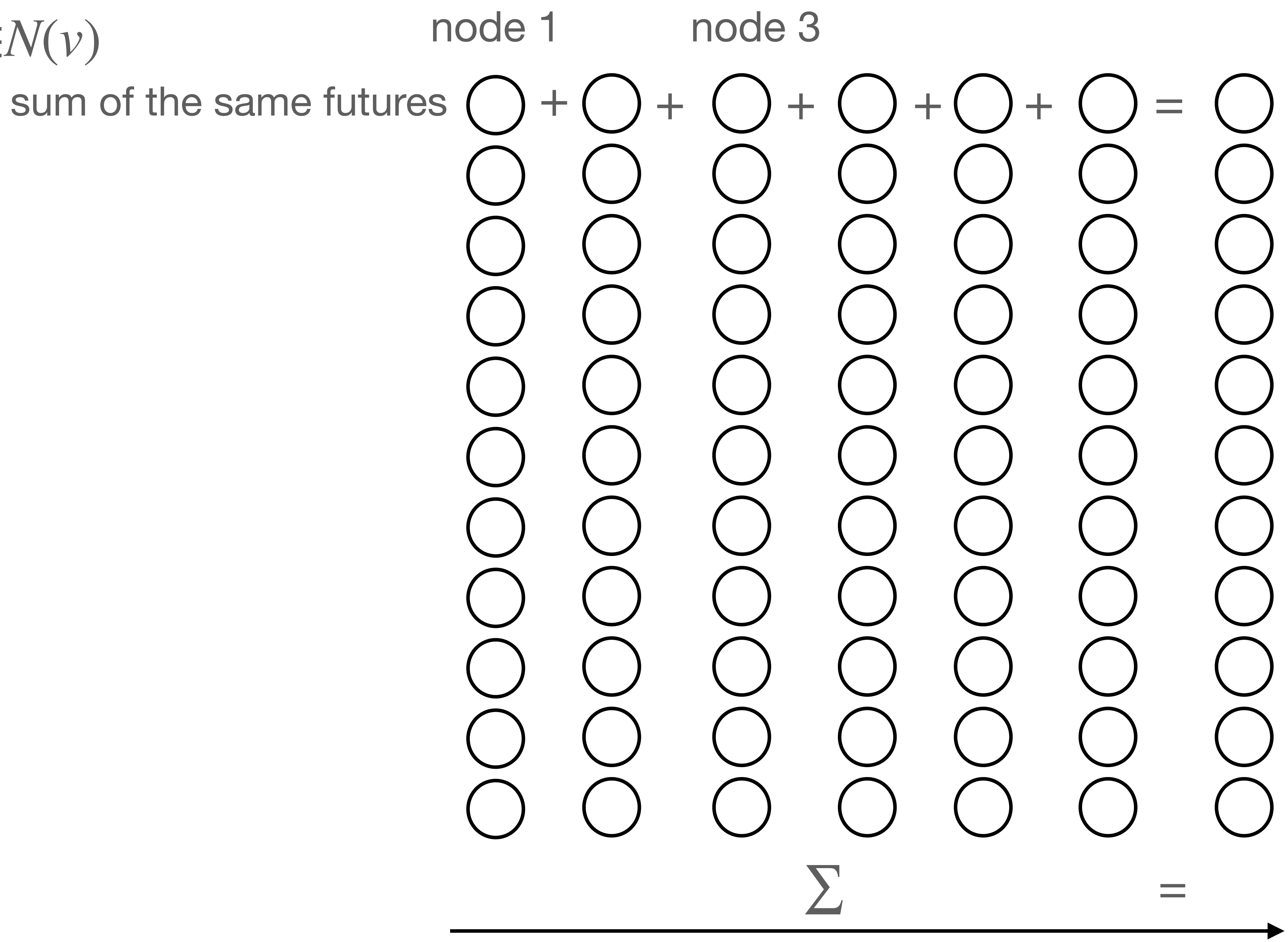

Graph Convolution Network:

$$h_v^{(k)} = f^{(k)}(W^{(k)} \cdot \frac{\sum_{u \in N(v)} h_u^{(k-1)}}{|N(v)|} + B^k \cdot h_v^{(k-1)})$$

$h_v^{(k)}$: embedding of node v

$|N(v)|$: the number of node v neighbours

For each step k, the function $f^{(k)}$, matrices $W^{(k)}$ and $B^{(k)}$ are shared across all nodes.

Graph Attention Network

$$h_v^{(k)} = f^{(k)}(W^{(k)} \cdot [\sum_{u \in N(v)} \alpha_{vu}^{(k-1)} h_u^{(k-1)} + \alpha_{vv}^{(k-1)} h_v^{(k-1)}])$$

$$\alpha_{vu}^{(k)} = \frac{A^{(k)}(h_v^{(k)}, h_u^{(k)})}{\sum_{w \in N(v)} A^{(k)}(h_v^{(k)}, h_w^{(k)})}$$

For each step k, the function $f^{(k)}$, matrices $W^{(k)}$ and attention mechanism $A^{(k)}$ (generally, another neural network) are shared across all nodes.

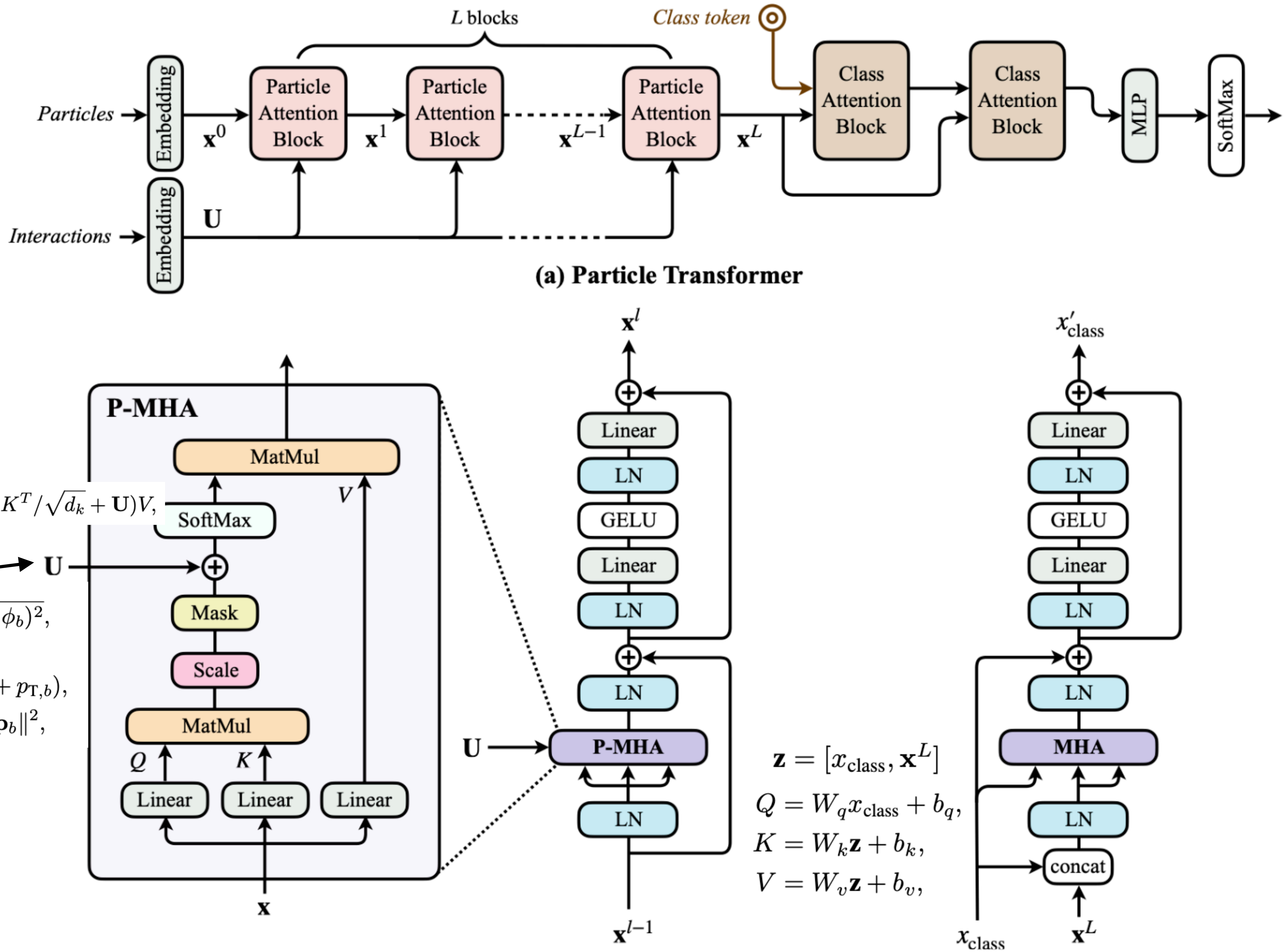

$$\text{P-MHA}(Q,K,V) = \text{SoftMax}(QK^T/\sqrt{d_k} + \mathbf{U})V,$$

$$\Delta = \sqrt{(y_a - y_b)^2 + (\phi_a - \phi_b)^2},$$
$$k_\text{T} = \min(p_{\text{T},a}, p_{\text{T},b})\Delta,$$
$$z = \min(p_{\text{T},a}, p_{\text{T},b})/(p_{\text{T},a} + p_{\text{T},b}),$$
$$m^2 = (E_a + E_b)^2 - \|\mathbf{p}_a + \mathbf{p}_b\|^2,$$

$$\mathbf{z} = [x_\text{class}, \mathbf{x}^L]$$
$$Q = W_q x_\text{class} + b_q,$$
$$K = W_k \mathbf{z} + b_k,$$
$$V = W_v \mathbf{z} + b_v,$$

(a) Particle Transformer

(b) Particle Attention Block

(c) Class Attention Block

Introduction of adiabatic quantum computation and the evolution from AQC to QAOA

AQC : a theoretical framework

components : 1, the driver Hamiltonian (H_D) encodes some quantum state that is easy to prepares its ground state 2, the problem Hamiltonian (H_P) encodes a quantum state we are interested in as its ground state

the idea underline the AQC : we start with a ground state that is easy to prepare and wish to end up with the quantum state we are interested in. This transition is accomplished via the adiabatic theorem, which states that a system in the ground state of some Hamiltonian will remain in the ground state if the Hamiltonian is changed slowly enough.

the process of AQC : 1, define the Hamiltonian: $H(t) = (1 - s(t))H_D + s(t)H_P$ and let our quantum system evolve under it. Unfortunately, time evolution under this time-dependent Hamiltonian involves very messy integral that is hard to evaluate : $U(t) = \tau e^{\frac{-i}{\hbar}\int_o^t H(T)dT}$

2, **We discretize $U(T)$ into intervals of Δt small enough that the Hamiltonian is approximately constant over each interval.**

3, Let $U(b, a)$ represent time evolution from time a to time b

$$U(T,0) = U(T, T - \Delta t)U(T - \Delta t, T - 2\Delta t)\dots U(\Delta t,0) = \prod_{j=1}^{P} U(j\Delta t, (j-1)\Delta t) \approx \prod_{j=1}^{P} e^{-iH(j\Delta t)\Delta t}$$

since $H(j\Delta t) = (1 - s(j\Delta t))H_D + s(j\Delta t)H_P$ **we get** $U(T,0) \approx \prod_{j=1}^{P} e^{-i(1-s(j\Delta t))H_D\Delta t} e^{-is(j\Delta t)H_P\Delta t}$

Thus we can approximate AQC by repeatedly letting the system evolve under H_P for some $s(j\Delta t)\Delta t$ and then H_D for some small $(1 - s(j\Delta t))\Delta t$

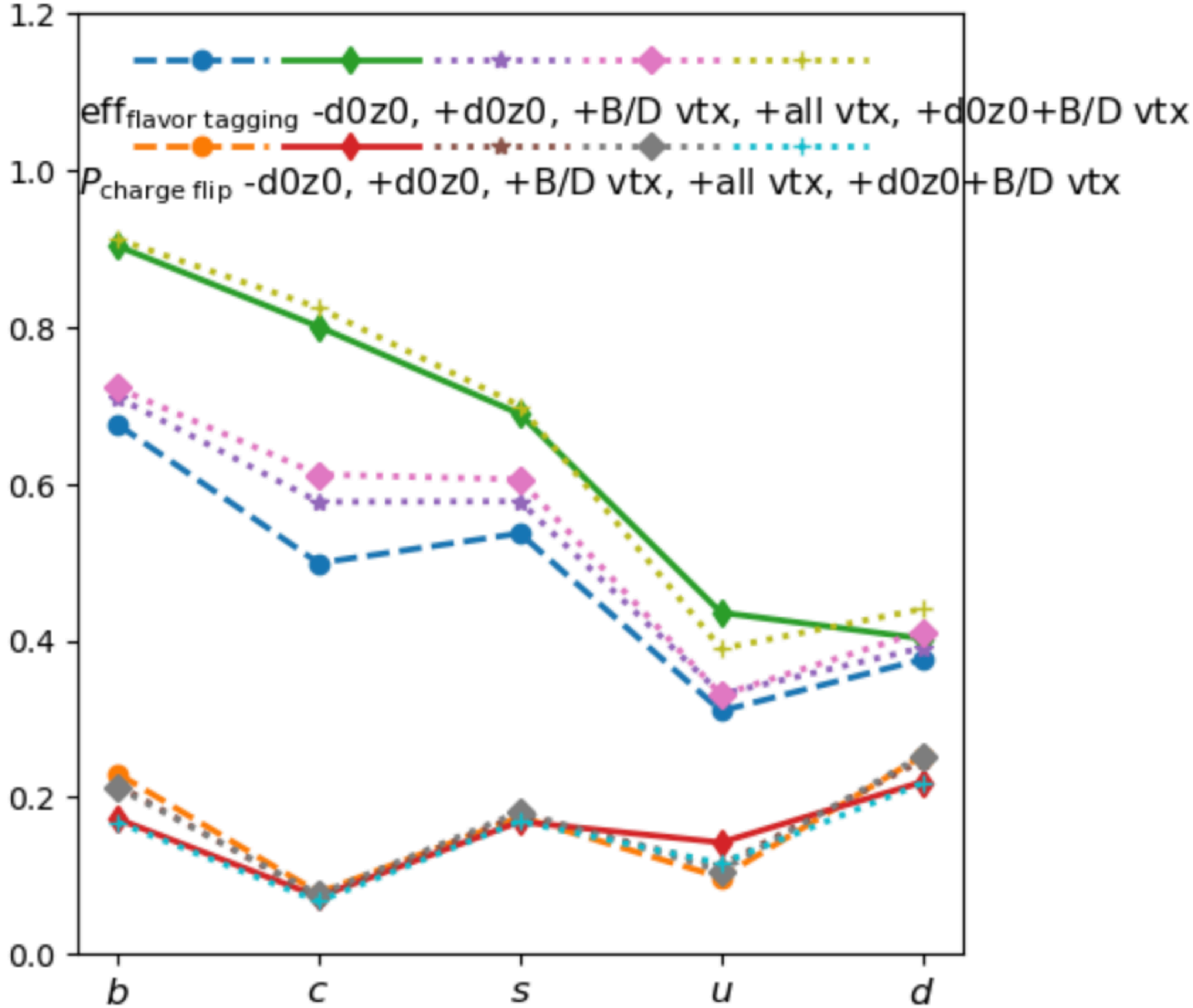

1.2
1.0
0.8
0.6
0.4
0.2
0.0
eff_flavor tagging -d0z0, +d0z0, +B/D vtx, +all vtx, +d0z0+B/D vtx
P_charge flip -d0z0, +d0z0, +B/D vtx, +all vtx, +d0z0+B/D vtx
b
c
s
u
d

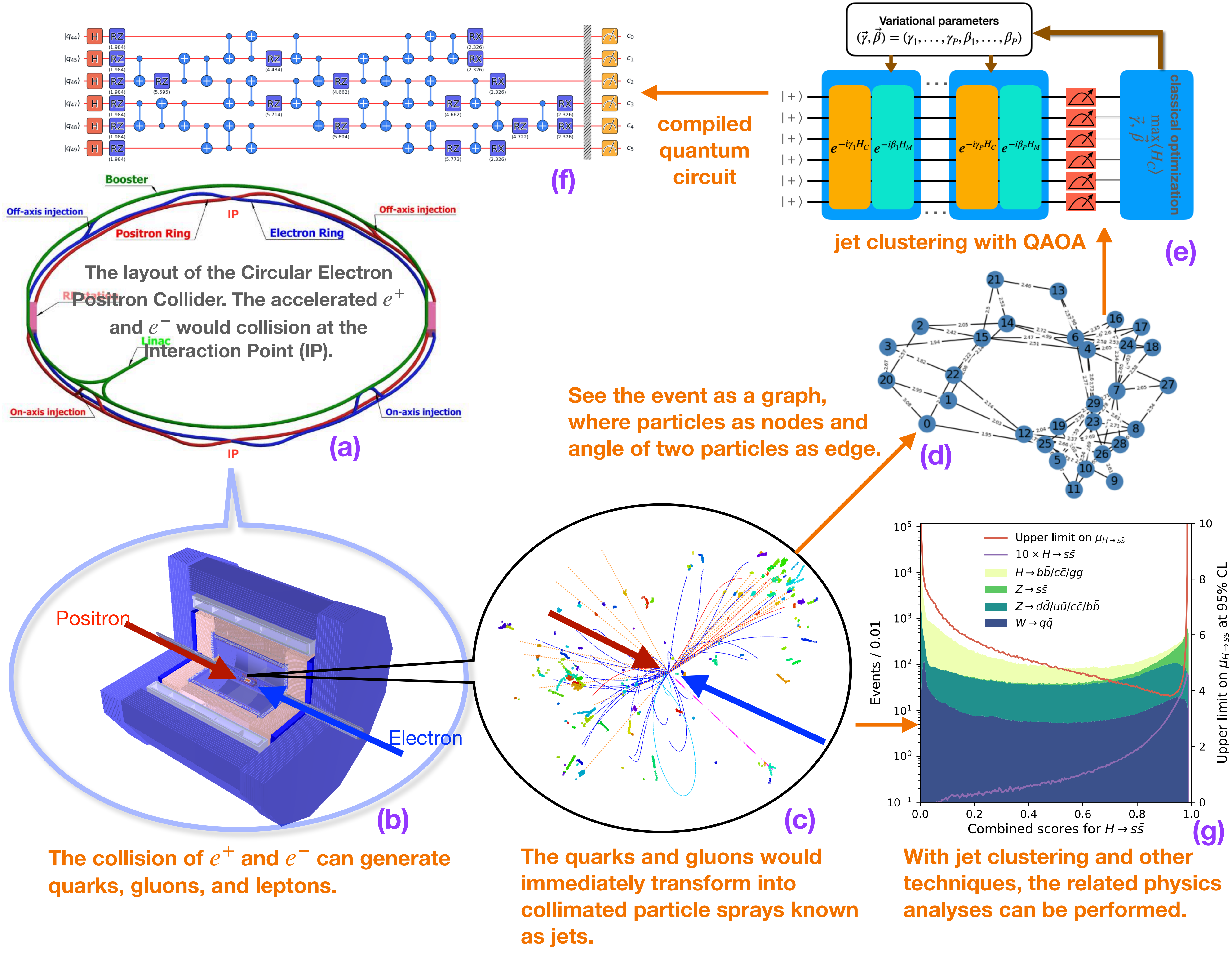

Variational parameters
$(\vec{\gamma}, \vec{\beta}) = (\gamma_1, ..., \gamma_P, \beta_1, ..., \beta_P)$
$e^{-i\gamma_1 H_C}$
$e^{-i\beta_1 H_M}$
$e^{-i\gamma_P H_C}$
$e^{-i\beta_P H_M}$
classical optimization
$\max_{\vec{\gamma}, \vec{\beta}} \langle H_C \rangle$
jet clustering with QAOA
(e)
compiled quantum circuit
(f)
Booster
Off-axis injection
IP
Positron Ring
Electron Ring
Off-axis injection
The layout of the Circular Electron Positron Collider. The accelerated e^+ and e^- would collision at the Interaction Point (IP).
Linac
On-axis injection
On-axis injection
IP
(a)
See the event as a graph, where particles as nodes and angle of two particles as edge.
(d)
Positron
Electron
(b)
(c)
Upper limit on $\mu_{H \to s\bar{s}}$
$10 \times H \to s\bar{s}$
$H \to b\bar{b}/c\bar{c}/gg$
$Z \to s\bar{s}$
$Z \to d\bar{d}/u\bar{u}/c\bar{c}/b\bar{b}$
$W \to q\bar{q}$
Events / 0.01
Upper limit on $\mu_{H \to s\bar{s}}$ at 95% CL
Combined scores for $H \to s\bar{s}$
(g)
The collision of e^+ and e^- can generate quarks, gluons, and leptons.
The quarks and gluons would immediately transform into collimated particle sprays known as jets.
With jet clustering and other techniques, the related physics analyses can be performed.